

Advances in Geosciences
Vol. 16: Atmospheric Science (2008)
Eds. Jai Ho Oh *et al.*
© World Scientific Publishing Company

SINGULAR VECTOR AND ENSO PREDICTABILITY IN A HYBRID COUPLED MODEL*

XIAOBING ZHOU^{†,‡} and YOU MIN TANG^{†,§}

[†]*Environmental Science and Engineering,
University of Northern British Columbia,
3333 University Way, Prince George, BC, V2N 4Z9, Canada*
[§]*ytang@unbc.ca*

[‡]*Centre for Australian Weather and
Climate Research (CAWCR), Bureau of Meteorology,
700 Collins St, Melbourne, VIC 3001, Australia*

In this study, singular vector (SV) and retrospective ENSO (El Niño and Southern Oscillation) predictions were performed respectively for the period from 1876 to 2000 using a hybrid coupled model. Emphasis was placed on exploring the relationship between SV and ENSO predictability. It is found that a defined Niño3 index from the first singular vector of sea surface temperature anomaly (SSTA) is highly correlated with the predicted Niño3 SSTA index of 6-month leads and that the first singular value (FSV) is positively correlated with the predictive skill. These results and findings improve our knowledge and understanding to the relationship between SV and predictability. It was thought that the fastest growth rate of errors to be inversely related to the prediction skill. The reasons why there is such a relationship between SV and realistic predictability include: (1) the strong signals of ENSO variability that favour the growth of initial uncertainties also have significant contributions to the predictability; (2) the averaged climate state of the tropical Pacific Ocean simultaneously effects both SV and predictability.

1. Introduction

The earliest report on the singular vector can be found in Lorenz's paper (1965) which introduced singular vector (SV) analysis into meteorology to study atmospheric predictability [1]. However, SV analysis had not been used to investigate ENSO predictability until the 1990s. Since then a lot of work has been approached on ENSO predictability studies using SV (e.g., Blumenthal 1991; Xue *et al.*, 1997a,b; Chen *et al.*, 1997; Thompson

*This work was supported by Canadian Foundation for Climate and Atmospheric Sciences grant to Y. Tang.

1998; Moore *et al.* 1996, 1997a,b, 2003; Fan *et al.*, 2000; Tang *et al.*, 2006; Zhou *et al.*, 2007) [2–13]. Despite different coupled models and norms used, these researches derived similar findings and conclusions such as: (1) the optimal initial and final patterns have large-scale features in the tropical Pacific Ocean. The initial pattern is insensitive to initial conditions while the final pattern depends on initial conditions; (2) the perturbation growth in coupled models is usually controlled by one dominant growing mode and its final pattern resembles ENSO-like pattern; (3) the optimal growth rates vary with the seasonal cycle and the phase of ENSO.

A wide perception in ENSO predictability and SV is an inverse relationship existing between them, namely, when the leading singular value is large, the predictability is low and vice versa (e.g., Moore *et al.*, 1996) [7]. The physical interpretation behind the perception is that the largest singular value describes the fastest growth rate of errors based on the definition of SV. Such an understanding and recognition to SV and ENSO predictability has been widely accepted. However, this theoretical perception has not been validated effectively using real ENSO prediction skill and SV because a long-term retrospective ENSO prediction and SV analysis was not available due to the limited length of observations, leading to difficulties to drive stable and robust conclusions and findings. Almost all SV analyses have to date, focused on a period around 20–30 years (e.g., Xue *et al.*, 1997b; Fan *et al.*, 2000) [4,11]. Recently we performed a long-term retrospective ENSO events and SV analysis for over 100 years from 1876–2000 (Zhou *et al.*, 2009) [14], which allows us to examine the relationship between SV and real predictability.

The motivation of this work is related to some recent studies on ENSO predictability. It has been found that ENSO predictability is highly dependent on the strength of ENSO variability. As the anomalies (signals) present in initial conditions are strong, the predictions are likely to be reliable (e.g., Chen *et al.*, 2004; Tang *et al.*, 2005; Tang *et al.*, 2007) [18, 13]. On the other hand, large singular values are also often associated with large anomalies. Thus the relationship between SV and predictability is most likely complicated, and probably unable to be simply characterized by the aforementioned theoretical perception. A detailed examination from long-term real prediction and SV analysis should be required.

In this paper, we will explore the relationship between predictability and SV through real prediction and SV for the past 125 years (1876–2000). Emphasis will be placed on the decadal variations in the predictability and in the SV. This paper is structured as follows: the model is introduced in

Sec. 2; the results on SV and ENSO predictability as well as their decadal variations will be presented in Sec. 3; finally a discussion and conclusion can be found in Sec. 4.

2. The Hybrid Coupled Model and the Computation of Singular Vector

The Hybrid Coupled Model (HCM) used in this study is composed of a nonlinear dynamical ocean model and a nonlinear empirical atmospheric model, identical to Tang (2002) and Zhou *et al.* (2007) [18, 13]. The ocean model is one of intermediate complexity, derived from Anderson and McCreary (1985) and Balmaseda *et al.* (1994, 1995) and extended to six activate layers [19, 20-21]. It covers the tropical Pacific Ocean 30°N–30°S in latitude and from 123°E–69°W in longitude with a horizontal resolution of $1.5^\circ \times 1.5^\circ$, and consist of the depth averaged primitive equations in six layers (with reference thickness of 100 m, 175 m, 250 m, 320 m, 400 m and 500 m from top to bottom). The atmospheric model is built by the nonlinear regression method, a neural network (NN).

The SVs were calculated using the tangent linear model (TLM) and Adjoint Model (AM) of the HCM ARPACK (ARnoldi PACKage) software package (Lehoucq *et al.*, 1998) based on the Lanczös algorithm was used to solve the singular value problem [22]. A L_2 -norm is adopted for the computation of SVs in this study. Details of the SVs computation can be found in Zhou *et al.* (2007) [13].

3. Result Analysis

The ocean model was forced by the reconstructed wind stress and integrated for 125 years from 1876 to 2000 (Zhou *et al.*, 2009) [14]. The observed SSTA –ERSST data (Extended Reconstructed SST; Smith and Reynolds, 2003, 2004 [23–24]) was assimilated into the oceanic model, leading to good ENSO simulation and predictions up to lead times of 12 months from 1876–2000 (Zhou *et al.*, 2009) [14]. The correlation between analyzed Niño3 SSTA index and the observed counterpart is up to 0.98 at the past 125-year period. The SV and each prediction were performed from same initial conditions, at a three-month interval starting from April 1, 1876 to January 1, 2001. This coupled model was able to successfully predict the major ENSO signals at a 6-month lead in the past 125 years. Hence we

will focus on the ENSO prediction at a 6-month lead and SV at a 6-month optimal period in following analysis.

3.1. Singular vector and predictability

The first singular vector (SV1) has the largest singular value that is much larger than others. Its typical spatial distribution in this coupled model consists of an east-west dipole spanning the entire tropical Pacific basin (not shown), which is similar to those of previous researches (e.g., Chen *et al.*, 1997; Xue *et al.*, 1997a; Zhou *et al.*, 2007) [5, 3, 14]. As can be seen in Fig. 1, the positive maximum center in SV1 along the equator moves eastward during El Niño and westward during La Niña. Its moving track is similar to the continuous redistribution of the warm surface waters. These waters are driven westward by intense westward trade wind during La Niña, and eastward by relaxed winds during El Niño (Fedorov and Philander, 2000) [25].

To study the relationship between SV1 and predictability, we defined a Niño3 SV1 index similar to the traditional Niño3 SSTA index, i.e. the averaged SV1 over Niño3 region. This region has the strongest interannual variability, and the largest forecast error growth in ENSO models. Thus, the SV1 index reflects well the variation in strength of SV1 pattern with time. Figure 2 shows the variation of Niño3 SV1 index and the predicted Niño3 SSTA index at a 6-month lead from 1876–2000. As can be seen, the Niño3 SV1 index is highly correlated with the predicted Niño3 SSTA at a 6-month lead with the correlation coefficient of 0.75 during the past 125 years. Furthermore, the variations of the amplitude of Niño3 SV1 index are closely associated with variations in the strength of ENSO events. For example, a strong ENSO event often has a large amplitude of Niño3 SV1 index and vice versa. Figure 2 sheds light on some important issues on SV: (1) the SV1 spatial pattern actually varies with initial conditions, as suggested by temporary variation of SV1 index, although its large scale structure is always characterized by the east-west dipole spanning the whole tropical Pacific for all initial condition like other models (e.g., Chen *et al.*, 1997; Xue *et al.*, 1997a,b; Zhou *et al.*, 2007) [5, 3-4, 13]; (2) the Niño3 region is a center of the dipole pattern of SV1, therefore Niño3 SV1 index measures the uncertainties most favourable for the error growth of prediction. Based on the concept of SV, a large value of Niño3 SV1 index should correspond with a poor prediction. However, it is not true here. As shown in Fig. 2, a large value of Niño3 SV1 index often corresponds with a good prediction. This is because a large Niño3 SV1 index often occurs at a strong ENSO event.

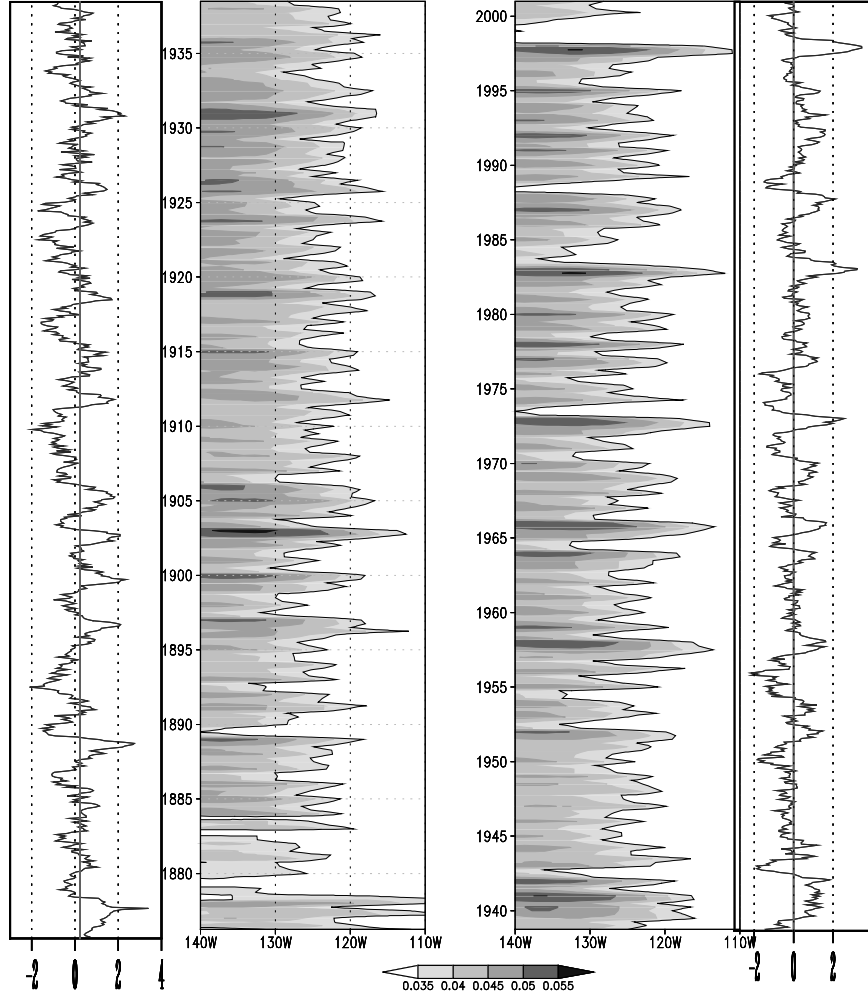


Fig. 1. Time-longitude diagram of the first singular vector (SV1) along the equator (shaded graphs) and the observed Niño3 SSTA index (line figures), from 1976-2000. Contour line in shaded graphs is 0.035°C and the values less than 0.035°C are blank in the SV pattern.

It has been found that the strength of ENSO signals significantly impact the prediction skill (Chen *et al.*, 2004; Tang *et al.*, 2005, 2007) [5, 16-17]. Therefore one should take caution to use SV to interpret predictability; (3) the Niño3 SV1 index can be used as a precursor for the ENSO event since it is quite consistent with the observed SSTA index of 6 months later.

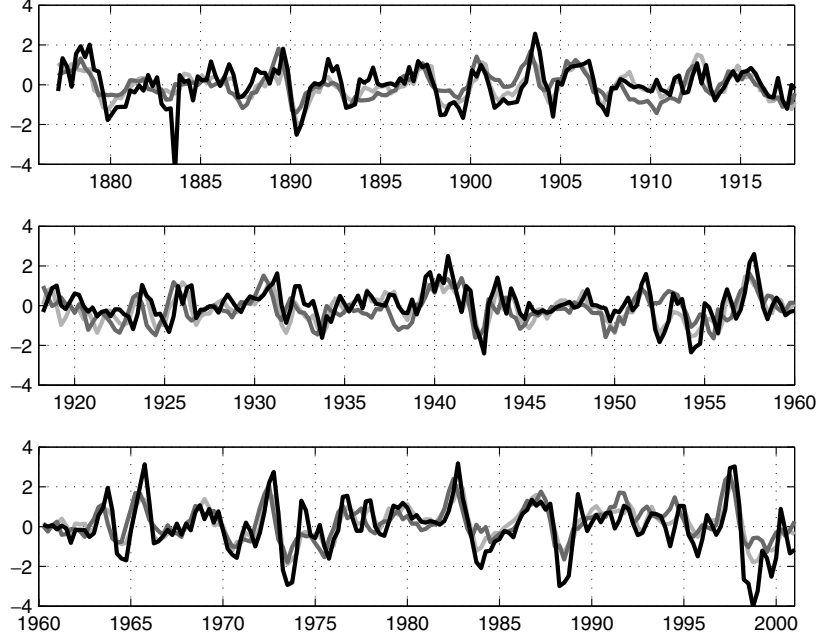


Fig. 2. Variations of the predicted Niño3 SSTA index of a 6-month lead (cyan), the observed Niño3 SSTA index (magenta) and normalized Niño3 SV1 index (black).

3.2. Singular value and predictability

3.2.1. Interdecadal variations of singular values

We have discussed SV1 in preceding section. In this section, we will turn to analyze the singular values, which reflect the optimal perturbation growth rates of initial uncertainties in a specified period. SVs are computed by adding small perturbations to the background state. The singular values are theoretically independent with perturbations but dependent on the background state with seasonal cycle, ENSO phase, and the decadal variability of ENSO. The previous studies only explored the impact of the seasonal cycle and ENSO phase on SVs in a relatively short period (e.g., Chen *et al.*, 1997; Xue *et al.*, 1997b; Moore and Kleeman, 1996; Tang *et al.*, 2006) [5, 4, 7, 12], which prohibited investigating the relationship between singular values and interdecadal variations of background mean state.

The 20-yr running mean of the first singular value (referred to as MSV1), model's spatial-average SST between 15°S–15°N (referred to as MSST) and the variance of Niño3 SSTA index (referred to as VNINO).

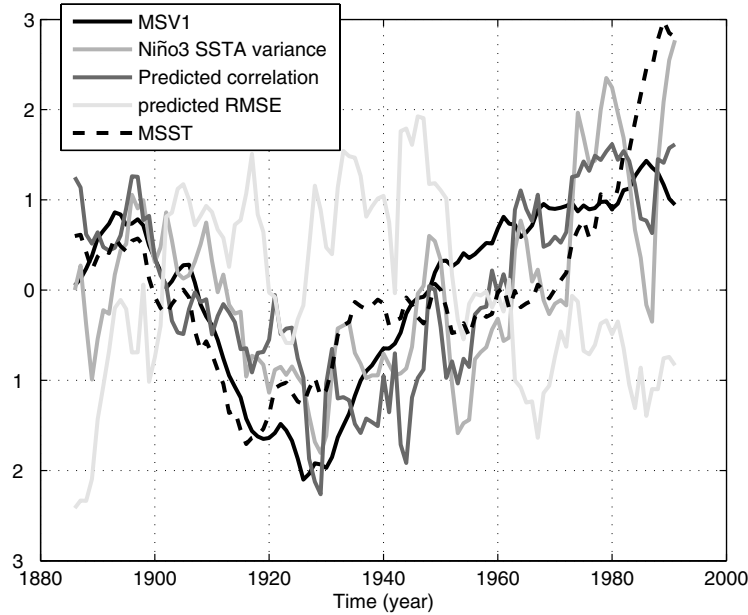


Fig. 3. Variation of the mean SST over 15° – 15° S and 123° E– 69° W, the variance (cyan) of Niño3 SSTA, MSV1 (solid black), predictive correlation (magenta) and RMSE (yellow) skill from 1876 to 2000. All were normalized prior to plotting.

This was obtained using 20-yr running windows,^a as is shown in Fig. 3. As can be seen, MSST reached a minimum in the 1920s, and then increased gradually till 1940. During the period from the 1940s to 1960s, it seemed stable. After the 1960s, MSST continuously increased, being consistent with the global warming. The correlation between MSST and VNINO is up to 0.68, indicating a good relationship between both. In other words, the signal strength (amplitude) and the mean state are highly related each other. The variation of MSV1 is in a very good agreement with that of MSST and VNINO. The good relationship between MSV1 and MSST (VNINO) is probably due to the fact that both were driven by the wind stress which showed significant interdecadal variations (not shown). Moore and Kleeman

^aWe calculate the skill in the first 20-yr window, saying from 1876–1895, denoted at 1885. Then we move the window forward one year, saying from 1877–1896, to calculate the skill again, denoted at 1886. This process will repeat until the skill is calculated in the last window, 1981–2000, denoted at 1990. Consequently, we can obtain a time series of 105 samples, which characterizes the decadal and interdecadal variations in prediction skills.

(1996) found that the first singular varied approximately in proportion to $|W|$ [7], a representative value of the mean wind speed, which acted as a coupling coefficient between the ocean and atmosphere. This is also true for the model used here. We found the singular values in this model are highly dependent on the coupling coefficient which determines the wind anomalies.

3.2.2. Interdecadal variations of singular value and predictability

In this subsection we will examine the relationship between decadal variation of the first singular value (FSV) and decadal variation of real prediction skill of ENSO, which is measured by correlation and root mean square error (RMSE) of predicted Niño3 SSTA index against the observed counterpart.

To study the interdecadal changes of prediction skills, the prediction skills are computed at each running window of 20-yr from 1876–2000. Figure 3 shows variations of the normalized correlation coefficient and RMSE at a 6-month lead from 1876–2000. As can be seen, the scores measured by RMSE are not always consistent with those by correlation (RMSE and correlation is quite different so they are always inconsistent). It is interesting to see that the trend of MSV1 is consistent with that of the correlation skill which has a correlation coefficient of 0.77. An inverse relationship also exists between MSV1 and RMSE and their correlation is -0.53 . This indicates that a large MSV1 has a high prediction skill and vice versa. Theoretically SV1 indicates the fastest growth rate of the initial uncertainties, leading to a lower prediction skill. However, the real situation in this model is totally different as the evidence above suggested. The reason is probably because strong signal anomalies (e.g., El Niño or La Niña) that control prediction skills also favour the growth of initial uncertainties. Some evidence can be found for this argument. For example, previous studies suggested that the final pattern of SV1, which described the final uncertainty growth, resembled the mature ENSO pattern. It should be noted that ENSO is the strongest interannual signal in the tropical Pacific Ocean. In Sec. 3.1, the Niño3 SV1 index is large before strong ENSO events and small before weak ENSO events. In Sec. 3.2, the variation of MSV1 follows well the variation of the strength of ENSO events. Therefore the contribution of stronger signal anomalies to predictability can be two sided. It can enhance predictability due to bringing more information or lowering predictability due to faster error growth. When the former exceeds the latter, a positive relationship between SV1 and predictability could be shown, as in Fig. 3. One should not understand their relationship as a

counterexample of the concept of SV. Instead, it should be interpreted as a net contribution of signal anomalies of ENSO variability to its predictability.

Figure 3 also shows that the change of the correlation skill is associated with the variation of MSST and VNINO. The correlation skill is lower during the relative “cold” period than that of “warm” period. The lowest correlation skill occurred around the 1930s, corresponding to the coldest period. Apparently the trend of the correlation skill is in good agreement with that of the MSST, and the fluctuation of the skill is consistent with that of VNINO. In general, a large VNINO will have relative high prediction skill, but this is not valid in some periods. For example, the “warm” period of the 1890s had relatively small VNINO but attained a high skill. This indicates that the correlation skill is determined by both MSST and VNINO. It can be taken as additional evidence to explain why MSV1 has a high positive relationship to correlation skill; because MSV1 is closely related to both MSST and VNINO.

4. Summary and Discussion

In this study, the ENSO predictability was explored based on singular values and prediction skills in the last 125 years from 1876 to 2000. The results show that the first singular vector actually varies with different initial conditions, although its large-scale feature along the equator is not sensitive to them. The positive maximum center of SV1 in the equatorial eastern Pacific moves westward during La Niña and flows back eastward during El Niño. The correlation coefficient between the Niño3 SV1 anomaly index and predicted Niño3 SSTA at a 6-month lead is up to 0.75 during a whole period of 1876–2000. Thus the Niño3 SV1 anomaly index can be used as a precursor of ENSO prediction.

The 20-yr running mean of the first singular value, measuring the mean growth rate of optimal initial perturbations in a 20-yr period, was calculated from 1876 to 2000. This running mean largely depends on the variation of 20-yr running means of model SST (MSST) and 20-yr-running variance of Niño3 SSTA index (VNINO). A large MSST will be possibly accompanied by a large MSV1 and vice versa.

The prediction skills are largely determined by both MSST and VNINO. The correlation skill is much lower during the “cold” period than during the “warm” period. The minimum correlation skill occurred in the coldest period of the 1930s. The fluctuations of correlation skill seem to

coincide with those of VNINO. Since MSV1 depends on MSST, a large MSV1 does not show a low correlation skill. On the contrary, a large MSV1 generally has a high correlation skill. The correlation coefficient between predictive correlation skill and MSV1 is up to 0.77 during the past 125 years.

Generally, model prediction skills are model dependent. A comparison of prediction skill between our model and Lamont's model (Zebiak and Cane, 1987; Chen, *et al.*, 2004) was examined [26, 15]. The result shows that the interdecadal variations of prediction skills in the two models are very similar (not shown), and both are consistent with the variations of MSST. This suggests these results found in our model might be applied to the other models.

The prediction skill in the last three decades is obviously higher than that in other periods. One might argue that this is because the coupled model used the data of these periods for training. We used a cross-validation scheme for any training, therefore artificial skill should be greatly alleviated although we cannot completely exclude it. Here we argue another factor, sea surface mean temperature in the tropical Pacific, plays an important role in attaining high prediction skill after the 1970s. The mean SST of the tropical Pacific increased significantly after the 1970s, corresponding with the climate regime shift in 1976. As evidenced in this study, the ENSO events are more predictable in the "warm" ocean than in the "cold" ocean, since the former is often associated with strong signals of *SST* variability leading to more information provided by predictions (Tang *et al.*, 2005) [16]. This also explains why both our model and Lamont's model had a good prediction skill during 1876 to 1900, when the mean SST was high.

Acknowledgments

We would like to thank Dr. Ziwang Deng for providing us with the reconstructed wind stress and helpful comments.

References

1. E. N. Lorenz, A study of the predictability of a 28-variable atmospheric model, *Tellus* **17** (1965) 321–333.
2. M. B. Blumenthal, Predictability of a coupled ocean–atmosphere model, *J. Climate* **4** (1991) 766–784.
3. Y. Xue, M. A. Cane and S. E. Zebiak, Predictability of a coupled model of ENSO using singular vector analysis. Part I: Optimal growth in seasonal background and ENSO cycles, *Mon. Weather Rev.* **125** (1997a) 2043–2056.

4. Y. Xue, M. A. Cane and S. E. Zebiak, Predictability of a coupled model of ENSO using singular vector analysis. Part II: Optimal growth and forecast skill, *Mon. Weather Rev.* **125** (1997b) 2057–2073.
5. Y.-Q. Chen, D. S. Battisti, T. N. Palmer, J. Barsugli and E. S. Sarachik, A study of the predictability of tropical Pacific SST in a coupled atmosphere–ocean model using singular vector analysis: The role of the annual cycle and the ENSO cycle, *Mon. Weather Rev.* **125** (1997) 831–845.
6. C. J. Thompson, Initial conditions for optimal growth in a coupled ocean–atmosphere model of ENSO, *J. Atmos. Sci.* **55** (1998) 537–557.
7. A. M. Moore and R. Kleeman, The dynamics of error growth and predictability in a coupled model of ENSO, *Quart. J. Roy. Meteorol. Soc.* **122** (1996) 1405–1446.
8. A. M., Moore and R. Kleeman, The singular vectors of a coupled ocean–atmosphere model of ENSO, II: Sensitivity studies and dynamical interpretation, *Quart. J. Roy. Meteorol. Soc.* **123** (1997a) 983–1006.
9. A. M. Moore and R. Kleeman, The singular vectors of a coupled ocean–atmosphere model of ENSO. Part 1: Thermodynamics, energetics and error growth, *Quart. J. Roy. Meteorol. Soc.* **123** (1997b) 953–981.
10. A. M. Moore, J. Vialard, A. T. Weaver, D. L. T. Anderson, R. Kleeman and J. R. Johnson, The role of air–sea interaction in controlling the optimal perturbations of low-frequency tropical coupled ocean–atmosphere modes, *J. Climate* **16** (2003) 951–968.
11. Y. Fan, M. R. Allen, D. L. T. Anderson and M. A. Balmaseda, How predictability depends on the nature of uncertainty in initial conditions in a coupled model of ENSO, *J. Climate* **13** (2000) 3298–3313.
12. Y. Tang, R. Kleeman and S. Miller, ENSO predictability of a fully coupled GCM model using singular vector analysis, *J. Climate* **19** (2006) 3361–3377.
13. X. Zhou, Y. Tang and Z. Deng, The impact of atmospheric nonlinearities on the fastest growth of ENSO prediction error, *Clim. Dyn.* (2007), doi:10.1007/s00382-007-0302-5.
14. X. Zhou, Y. Tang and Z. Deng, Assimilation of historical SST data for long-term ENSO retrospective forecasts, *Ocean Modelling* (2009).
15. D. Chen, M. A. Cane, A. Kaplan, S. E. Zebiak and D. Huang, Predictability of El Niño in the past 148 years, *Nature* **428** (2004) 733–736.
16. Y. Tang, R. Kleeman and A. Moore, On the reliability of ENSO dynamical predictions, *J. Atmos. Sci.* **62** (2005) 1770–1791.
17. Y. Tang, Z. Deng, X. Zhou, Y. Cheng and D. Chen, Interdecadal variation of ENSO predictability in multiple models, *J. Climate* **21** (2008) 4811–4833.
18. Y. Tang, Hybrid coupled models of the tropical Pacific? — Interannual variability, *Clim. Dyn.* **19** (2002) 331–342.
19. D. L. T. Anderson and J. P. McCreary, Slowly propagating disturbances in a coupled ocean–atmosphere model, *J. Atmos. Sci.* **42** (1985) 615–629.
20. M. Balmaseda, D. L. T. Anderson and M. K. Davey, ENSO prediction using a dynamical ocean model coupled to statistical atmospheres, *Tellus* **46A** (1994) 497–511.

21. M. Balmaseda, M. K. Davey and D. L. T. Anderson, Decadal and seasonal dependence of ENSO prediction skill, *J. Climate* **8** (1995) 2705–2715.
22. R. B. Lehoucq, D. C. Sorensen and C. Yang, *ARPACK Users' Guide* (SIAM, Philadelphia, USA, 1998).
23. T. M. Smith and R. W. Reynolds, Extended reconstruction of global sea surface temperatures based on COADS data (1854–1997), *J. Climate* **16** (2003) 1495–1510.
24. T. M. Smith and R. W. Reynolds, Improved extended reconstruction of SST (1854–1997), *J. Climate* **17** (2004) 2466–2477.
25. A. V. Fedorov and S. G. H. Philander, Is El Niño changing? *Science* **288** (2000) 1997–2002.
26. S. E. Zebiak and M. A. Cane, A model El Niño–Southern Oscillation, *Mon. Weather Rev.* **115** (1987) 2262–2278.